Materials and Structures (2025) 58:359
https://doi.org/10.1617/s11527-025-02883-8

ORIGINAL ARTICLE

Evaluation of admixtures from agricultural and aquacultural sources on hydration and mechanical properties of Portland cement based materials

Bright Asante · Luís Urbano Durlo Tambara · Montserrat Soria-Castro · Alejandra Ramírez · Pedro Castro-Borges · Wolfram Schmidt

Received: 2 June 2025 / Revised: 17 September 2025 / Accepted: 15 November 2025 / Published online: 29 November 2025

Abstract This study investigates the potential of bio-admixtures derived from *Sargassum natans* (SN1E, SN2E), *Sargassum fluitans* (SFE), water hyacinth (WHE), miscanthus grass (ME), and plantain stem (PSE) as sustainable alternatives to polycarboxylic ether (PCE) superplasticizers in cement-based materials. The research examines their effects on rheology, hydration, microstructure, and mechanical properties to assess their suitability for eco-friendly construction applications. Cement pastes and mortars incorporating 0.1% and 1% bio-admixture dosages were analyzed using isothermal calorimetry, thermogravimetric analysis (TGA/DTG), static yield stress measurements, and compressive strength testing at 7 and 28 days. Results indicate that all mixtures containing admixtures exhibited lower initial yield stress values, indicating a liquefying effect initially. At 0.1% dosage, the admixtures exhibited comparable or slightly improved compressive strength relative to the reference (REF), with no significant losses. However, at 1% dosage, PCE, WHE, ME, and PSE showed notable strength reductions, particularly ME, which significantly impaired both 7-day and 28-day strengths. Hydration studies revealed that bio-admixtures exhibited lower retardation effects compared to PCE, with SN1E, SN2E, and SFE promoting early hydration and portlandite (CH) formation. Conversely, ME and PSE exhibited delayed hydration, leading to lower early-age strengths but a more sustained hydration process over time. Thermal analysis further confirmed these trends, with bio-admixture-modified pastes maintaining stable hydration profiles, while PCE exhibited the strongest retardation effect, as evidenced by its lower total weight loss, and reduced CH content. These findings highlight the potential of bio-admixtures as sustainable modifiers in cementitious materials, providing workability benefits while minimizing hydration delay, making them promising candidates for green construction.

Keywords Bio-admixtures · Yield stress · Cement hydration · Compressive strength · Polysaccharides

B. Asante (✉) · L. U. Durlo Tambara · W. Schmidt
Bundesanstalt für Materialforschung und -prüfung (BAM), Unter den Eichen 87, 12205 Berlin, Germany
e-mail: bright.asante@bam.de

L. U. Durlo Tambara
e-mail: luis-urbano.durlo-tambara@bam.de

W. Schmidt
e-mail: wolfram.schmidt@bam.de

M. Soria-Castro · P. Castro-Borges
Departamento de Física Aplicada, Centro de Investigación y de Estudios Avanzados del Instituto Politécnico Nacional Unidad Mérida, Mexico, Mexico
e-mail: montserrat.soria@cinvestav.mx

P. Castro-Borges
e-mail: pcastro@cinvestav.mx

A. Ramírez
Energy Materials In-situ Laboratory at Helmholtz-Zentrum Berlin für Materialien und Energie, Berlin, Germany
e-mail: alejandra.ramirez-caro@helmholtz-berlin.de

1 Introduction

Sustainability has emerged as a fundamental principle in contemporary concrete technology, emphasizing the development of highly durable and environmentally sustainable construction materials with minimal ecological footprints [1]. As the most widely utilized construction material, concrete is undergoing significant advancements through the integration of sustainable practices and materials to align with global environmental objectives. Among these innovations, chemical admixtures have proven to be essential in modifying the properties of fresh concrete to achieve specific performance criteria, which also influence hardened concrete properties. However, most rheology-modifying admixtures to date are derived from petrochemical sources, characterized by complex global supply streams, high carbon dioxide emissions, and significant environmental footprints, including high water consumption. These challenges have driven interest in bio-based chemical admixtures as sustainable alternatives for environmentally friendly concrete production.

Among the various types of admixtures, superplasticizers (SPs) are among the most important due to their critical role in enhancing workability and reducing water content in concrete. Superplasticizers, such as polycarboxylate ethers (PCE), are widely used for high-performance concrete. These polymers consist of a polycarboxylic backbone and ethylene oxide graft chains, with adsorption mechanisms based on their interaction with clinker and hydration phases [2–8]. Upon adsorption, superplasticizers provide steric hindrance, to disperse cement particles and to improve rheological properties. The effectiveness of this process depends on the adsorption and resulting steric effect, which are influenced by the molecular structure of the polymer, particularly its charge density [9]. For example, PCEs primarily adsorb on aluminate and ferrite clinker phase surfaces and newly formed hydration phases, such as ettringite and monosulfate, during early hydration [2, 8]. However, this interaction mechanism is complex. Adsorption processes interfere with ion interactions in the solution and hinder the growth of newly formed crystals, leading to a delicate balance between the effects of polymers on rheology and cement hydration kinetics. Such interactions have significant implications for both early-age properties and the long-term performance of cementitious materials.

The molecular diversity of bio-admixtures introduces additional complexity. Biopolymers or admixtures derived from agricultural and aquacultural sources often exhibit intricate polymeric structures, which can influence their adsorption behavior, impact on rheological effects, and hydration. Unlike conventional superplasticizers, bio-admixtures may exhibit highly variable effects on rheology, slump life, and early hydration due to their unique chemical compositions, typically highly branched molecular structure and complex interactions with cement phases [10]. In addition, their effect may not only depend on the dosage but also on the solid particle volume fraction [11]. This complexity is further reflected in how admixtures mainly affect the rheology of cement-based materials. Choosing a type of admixture and a specific amount offers the possibility of adjusting the rheology according to specified performance criteria. Particularly accelerated or retarded setting can be observed [12–15]. These effects happen depending on their molecular architecture, dosage, and interaction with the pore solution chemistry [16, 17]. On the other hand, the adsorption of bio-admixtures on cement grains and hydration products may significantly influence hydration kinetics, setting times, and strength development. For instance, the steric hindrance effect of superplasticizers and their interaction with hydration phases, such as ettringite, can delay the accelerated hydration of calcium silicate hydrates (C-S-H) [2, 8].

Conventional admixtures like naphthalene sulfonated formaldehyde condensates and polycarboxylates are energy-intensive to produce and rely on non-renewable resources, contributing significantly to the overall environmental impact of concrete production [18–20]. In contrast, bio-based chemical admixtures, sourced from renewable agricultural and aquacultural materials, offer a sustainable alternative. Their local availability reduces CO_2 emissions associated with transportation and promotes local value chains, making them an eco-friendly option for concrete production. Many of these materials contain effective sugar-based polymers that can often be extracted through simple processes. Numerous plant-based materials have been investigated for their potential as rheology modifiers, demonstrating promising results in improving workability and hydration control. Examples

include *Acacia Karroo* gum [21], cassava and maize starches [22], arrowroot [19], corn [18], sugar molasses [23], aqueous okra extracts [24], and grape and mulberry extracts [1]. These bio-admixtures not only contribute to sustainability but also offer functional advantages, making them viable substitutes for conventional chemical admixtures.

The current research aims to advance the understanding of bio-based chemical admixtures derived from agricultural sources, such as plantain stem and miscanthus extracts, and aquacultural sources, including *Sargassum natans* (i.e., N I and N VIII), *Sargassum fluitans* (F III), and water hyacinth. The agricultural residues were selected for their abundance and potential as sustainable, locally available resources. In contrast, the aquacultural materials, notably Sargassum species and water hyacinth, were chosen due to their high invasiveness and associated environmental challenges in coastal and freshwater ecosystems. Utilizing these invasive species as feedstocks for bio-admixture production offers an opportunity to mitigate ecological problems while contributing to sustainable construction solutions. The study evaluates bio-based admixtures from these six residues to investigate their influence on the yield stress of cementitious systems, determining their potential as plasticizers. Additionally, their effects on the hydration process of Portland cement and the compressive strength of cement-based materials were systematically assessed as well as FTIR and ^{1}H-NMR characterization to determine which organic molecules are present in the bio-admixtures and which properties may be influencing the chemical processes of cement hydration.

2 Materials and methods

2.1 Materials

Ordinary Portland cement (CEM I 42.5 N) was used to produce the mortars and pastes. The bio-admixtures used in this study were derived from *Sargassum natans* N I and N VIII (SN1E and SN2E), *Sargassum fluitan* F III (SFE), miscanthus grass (ME), water hyacinth "*Pontederia crassipes*" (WHE), and plantain stem (PSE). Additionally, powder-type polycarboxylic ether (Melflux AP 101) was used as a reference admixture. Figure 1 presents the XRD patterns of the bio-admixtures. Sylvite (KCl) reflections were identified in all the bio-admixtures, with small pattern intensities for ME and PSE. Extracts from the three sargassum species and the water hyacinth predominantly consisted of sylvite and halite (NaCl) salts. The miscanthus grass (ME) contained sylvite, weddellite ($CaC_2O_4{\cdot}2H_2O$), potassium hydrogen carbonate

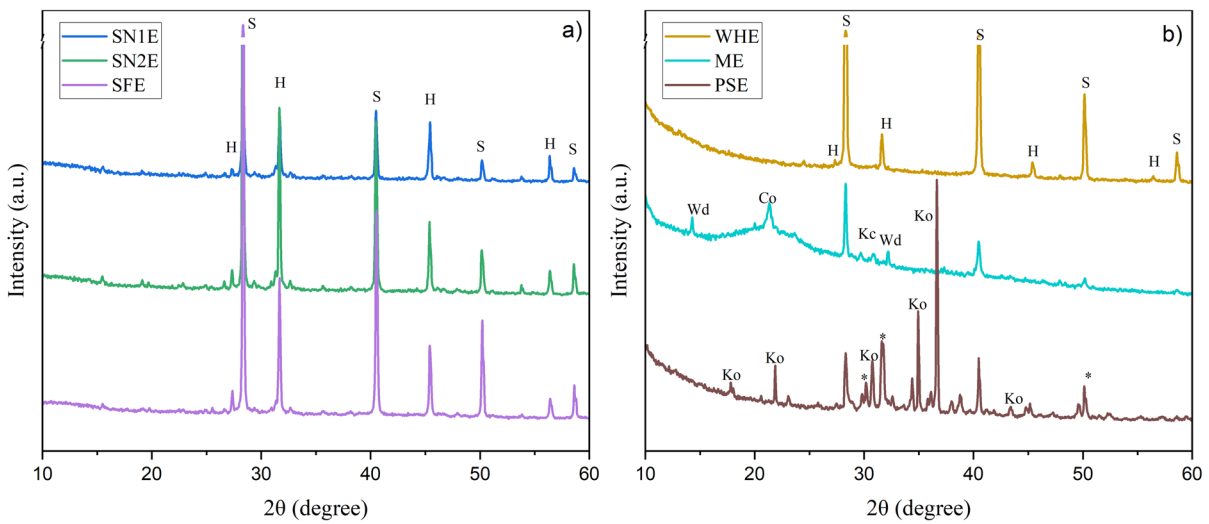

Fig. 1 XRD patterns of the bio-admixture materials: **a** Sargassum species and **b** water hyacinth, miscanthus, and plantain stem. Identified phases are indicated as (H: halite; S: sylvite; Wd: weddellite; Co: calcium oxychloride; Kc: potassium hydrogen carbonate hydrate ($K_4H_2{\cdot}(CO_3)_3{\cdot}1.5H_2O$); Ko: potassium oxalate hydrate oxide ($K_2C_2O_4H_2O$); *: K_3OCl)

hydrate ($K_4H_2{\cdot}(CO_3)_3{\cdot}1.5H_2O$), and calcium oxychloride ($3CaO{\cdot}CaCl_2{\cdot}21H_2O$). The plantain stem (PSE) included sylvite, potassium hydrogen carbonate hydrate, potassium oxalate hydrate, and potassium oxide chloride (K_3OCl).

2.2 Extraction of bio-admixtures and sample preparation

Figure 2 illustrates the extraction process for the organic bio-admixtures. Dry material from the organic sources was mixed with water at a 1:20 ratio and heated to 80 °C for 30 min. After heating, the mixture was filtered to separate the solid residue from the liquid extract. Since organic extractives are stable at temperatures between 60 and 100 °C [25, 26], the liquid extract was dried in an oven at 60 °C for 72 h. The resulting solid extracts were then collected and ground into a fine powder.

Mortar specimens were prepared to determine the mechanical and yield stress. The cement/aggregate ratio to manufacture the mortars was 1:2.35, with a constant water-to-cement (W/C) ratio of 0.56. A standardized 0.1/0.5 mm siliceous sand was employed. The powdered bio-admixtures and the polycarboxylate ether (PCE) were added at 0.1% or 1.0% of the water weight (dosages expressed relative to water were chosen since viscosity-modifying admixtures primarily act on the aqueous phase). As a reference, samples without any admixtures were also prepared for comparison.

All mixtures were dry-mixed (sand, cement, and any admixtures) for 2 min at 250 rpm. Water was then added, mixing continued for another 2 min at 250 rpm, followed by 1 min at 400 rpm, before casting and testing. For calorimetry, XRD, and TGA, cement paste samples with the same W/C ratio were prepared and cured for 7 or 28 days prior to testing.

2.3 Physicochemical behavior of PCE and bio-admixtures in aqueous and alkaline media

To assess the behavior of the PCE and bio-admixtures in different environments, their particle size (Z-Average) and surface charge (Zeta potential) were measured using a Malvern Zetasizer Nano at 25 ± 0.5 °C. The pH was measured just before the zeta potential tests to better understand the chemical environment of each dispersion. Samples were prepared in deionized water and in a 0.01 M calcium hydroxide solution, with each polymer dispersed at 0.01% (w/v). The dispersions were vortexed for 1 min to ensure proper mixing, then filtered through 0.45 µm syringe filters to remove any large particles or bubbles before testing. The average values from triplicate measurements are presented in Table 1.

2.4 Experiment

2.4.1 FTIR and ^{1}H-NMR analysis

The NMR experiments were conducted at 25 °C in a 600 MHz Varian-Agilent AR Premium Compact (14.1 T) (WHE, ME and PSE) and a 500 MHz Bruker Avance III (11.75 T) (SN1E, SN2E, and SFE). Approximately 5 mg of each extract were dissolved in 700 µL of D_2O (0.05% TSP as reference for chemical shift) and transferred to a 5 mm NMR tube. The ^{1}H-NMR were recorded using a water presaturation sequence (PRESAT for Varian and zgf2pr for Bruker) with 128 transients collected in 65 k data points. The resulting spectra were manually phased, and baseline

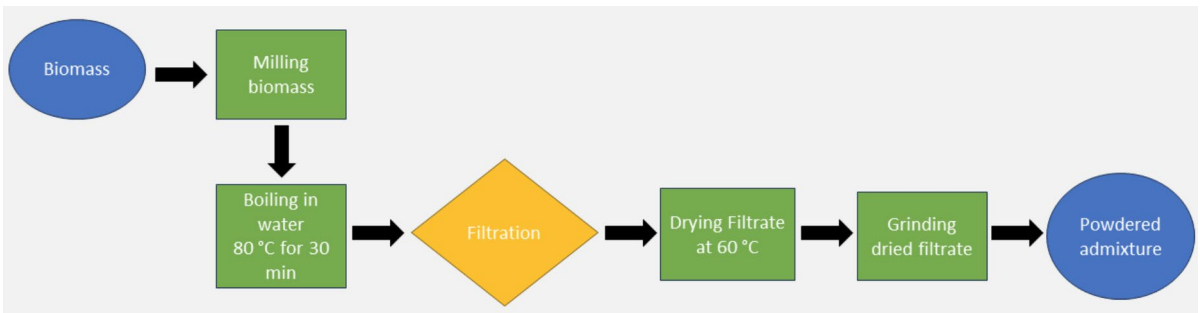

Fig. 2 Extraction process of bio-admixtures from agriculture and aquaculture resources

Table 1 Average size, pH and zeta potential of admixtures in aqueous and alkaline media

Sample	Average size (nm)		pH		Zeta potential (mV)	
	Water	$Ca(OH)_2$	Water	$Ca(OH)_2$	Water	$Ca(OH)_2$
PCE	63.83 ± 0.9	172.10 ± 0.9	7.96 ± 0.02	12.38 ± 0.03	− 9.26 ± 4.3	− 5.11 ± 0.2
SN1E	198.63 ± 1.6	188.87 ± 1.2	9.13 ± 0.02	12.31 ± 0.02	− 30.13 ± 1.2	− 16.43 ± 0.9
SN2E	183.50 ± 5.1	165.17 ± 1.5	9.15 ± 0.08	12.31 ± 0.02	− 27.13 ± 2.0	− 19.50 ± 1.35
SFE	175.27 ± 2.30	175.27 ± 1.9	10.16 ± 0.04	12.30 ± 0.01	− 29.90 ± 0.6	− 17.77 ± 1.8
WH	176.97 ± 3.7	213.63 ± 4.8	8.49 ± 0.02	12.35 ± 0.03	− 21.93 ± 1.4	− 15.10 ± 0.2
ME	108.93 ± 2.1	155.37 ± 3.9	9.81 ± 0.04	12.34 ± 0.01	− 22.33 ± 1.0	− 14.30 ± 0.7
PSE	122.03 ± 2.2	407.17 ± 10.6	10.37 ± 0.02	12.36 ± 0.02	− 34.20 ± 1.0	− 19.20 ± 1.7

corrected using MNova (Mestrelab Research SL, Santiago de Compostela, Spain); an exponential function with a line broadening factor of 0.3 Hz was applied and the reference set to TSP (δ0.00).

FTIR spectra were obtained using a Thermo Scientic Nicolet iS5 FTIR spectrometer in ATR (iD7) mode with 64 scans and a resolution of 8 cm^{-1} in the wavenumber region from 4000 to 500 cm^{-1}.

2.4.2 *Yield stress testing*

A conical penetrometer (Brookfield AMETEK CT3-100-115 LFRA) with a 24 mm diameter, a cone tip angle of 30°, and a height of 44.78 mm (Fig. 3) was used for the tests. A fast penetration method was applied, with a constant loading rate of 0.5 mm/s until 8 mm penetration depth was achieved. The fresh mortar samples, prepared and cast into 20 mm cubes, were tested with a penetration depth of 8 mm to minimize resistance from the bottom of the samples. Preliminary trials with 20 mm cube, 50 mm × 30 mm cylinder, and 55 mm × 18 mm cylinder (diameter x height) showed no big difference in penetration results at the same depth when the same cone was used, confirming the suitability of the 20 mm cube mold. This choice minimized material wastage and allowed one sample to be tested per fresh mortar cube. The trigger point for starting the measurements was set at 1 g. Since the load-bearing surface of the cone remains constant during penetration and is independent of penetration depth [27], the method reduces sensitivity to edge effects provided penetration does not exceed more than half of the sample height.

Measurements were taken at 0, 15, 30, 45, and 60-min intervals for each mortar sample. The initial tests were conducted approximately 5 min after the

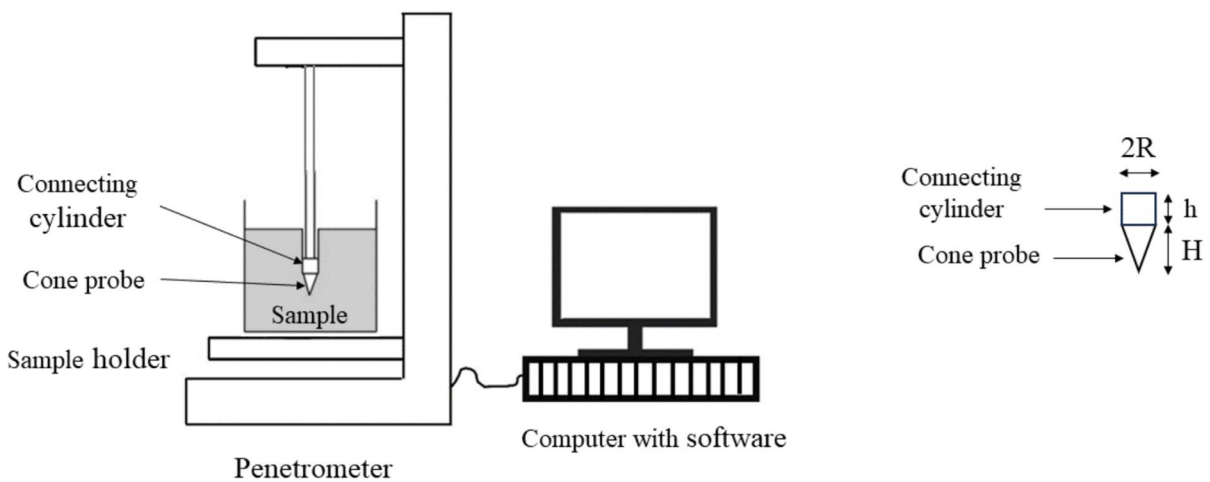

Fig. 3 Schematic drawing of texture analyzer for the penetration test (not to scale)

addition of water during mixing, recorded as time 0. After each test, the penetrometer was cleaned with a wet cloth, followed by a dry cloth. In line with the method described by Lootens et al. [27], the static yield stress (τ0) was calculated using Eq. 1.

$$\tau_0 = \frac{F}{\pi R\left(\sqrt{R^2 + H^2} + 2h\right)} \quad (1)$$

In this equation, τ_0 represents the static yield stress, F is the maximum penetration force within the 8 mm penetration depth, R is the cone radius, H is the cone height, and h is the height of the corresponding cylinder (Fig. 3).

2.4.3 Compressive strength testing

Before the strength tests, the samples were cured in water until the age of testing. Compressive strength was measured using a ToniPRAX device, in accordance with DIN EN-196-1:2019. To account for the specimen dimensions (20 mm × 20 mm × 20 mm), the loading rate was reduced to one-tenth of the standard rate (240 N/s). Tests were conducted at 7 and 28 days, with the average compressive strength calculated from three replicates at each age. The corresponding standard deviations are also reported.

2.4.4 Calorimetry

The heat flow and total heat released during hydration reactions were measured using isothermal conduction calorimetry, following DIN EN 196-11 standards. The tests were conducted with a Thermometric TAM AIR calorimeter at a constant temperature of 20 °C over 170 h. Quartz sand was used as a reference. For each sample, 25.95 g of cement, 14.65 g of water, and 0.15 g of admixture were used. The dry cement and admixture were mixed at 250 rpm for 1 min, after which the water was added and mixed for an additional 2 min. Immediately after mixing, 14 g ± 0.5 of the paste was placed into an ampoule and transferred to the calorimeter. The time from water addition to the start of measurement was approximately 5 min. A reference sample without admixture was also prepared for comparison. Following calorimetric measurements, samples were kept in plastic containers for microstructural evaluation at 7 and 28 days (Sect. 2.4.5). Consequently, a certain degree of carbonation was unavoidable, with a more pronounced effect expected in the 28-day samples.

2.4.5 XRD and TGA

Prior to conducting the XRD and TGA analyses, the hydration of cement pastes was stopped after 7 and 28 days of curing. This was achieved by manually crushing fractured pieces of the samples and immersing them in 50 ml of isopropanol. The isopropanol was replaced at intervals of 3 h, 1 day, and 3 days. After 7 days, the pieces were rinsed using additional isopropanol on filter paper. Subsequently, the samples were dried at 40 °C for 24 h. Fine powders for XRD and TGA analyses were prepared by manually grinding the dried samples with a mortar and pestle.

XRD measurements were conducted using a BRUKER D2 phaser (2nd Gen) with Cu Kα radiation ($\lambda = 1.5419$ Å) in Bragg–Brentano geometry. The measurement parameters were set to 30 kV/10 mA for the cathode, with a 1 mm (0.95°) divergence slit. The scanning range was 5–70° 2θ, with a step size of 0.02° 2θ and a time per step of 1 s. Thermogravimetric analysis (TGA) was performed using a Mettler Toledo device. Approximately 10 mg of each sample was analyzed under flowing nitrogen gas, with a heating rate of 10 K/min from 40 to 1000 °C.

2.5 Portlandite (CH) content

Portlandite (CH) decomposes within the temperature range of 400–500 °C, forming CaO and H_2O [28, 29]. The weight loss ($WL_{Ca(OH)2}$) associated with the evaporation of water can be used to calculate the amount of Portlandite present. This calculation relies on the molecular masses of Portlandite ($M_{Ca(OH)2} = 74$ g/mol) and water ($M_{H2O} = 18$ g/mol). From the TGA analysis, the weight loss due to Portlandite decomposition was quantified over the range 380–500 °C using the tangential method [28, 29]. The precise temperature limits for the decomposition interval were determined based on the derivative of the mass loss curve (DTG). Using the formula below, the Portlandite (CH) content was calculated as weight percent (wt. %) of the sample:

$$CH(\%) = WL_{Ca(OH)_2} \times \frac{M_{Ca(OH)_2}}{M_{H_2O}} \quad (2)$$

where $WL_{Ca(OH)2}$ are the weight loss of the samples at approx. 380 °C, $M_{Ca(OH)2}$ is the molar weight of $Ca(OH)_2$, and M_{H2O} is the molar weight of H_2O.

Previous studies [30, 31] have determined the total Portlandite content by combining the mass loss associated with Portlandite dehydroxylation, as defined in Eq. (2), with the decarbonation mass loss observed around 700 °C, which corresponds to Portlandite that has transformed into calcite during storage or thermal analysis. In the present work, XRD analysis indicated that partial carbonation had already occurred during curing. Therefore, Eq. (2) was applied without incorporating the carbonate fraction, and only the Portlandite present in its non-carbonated ("fresh") form was quantified.

3 Results

3.1 FTIR and NMR

FTIR analyses (Fig. 4a, b) of bio-admixture materials revealed a variety of functional groups corresponding to diverse organic molecules; briefly, the bands around ~3200 and 2900 cm^{-1} are attributed to O–H and C–H stretching vibration, respectively, while absorptions between 1600 and 1400 cm^{-1} represent antisymmetric and symmetric vibration from carboxylate groups. The intense band at ~1023 cm^{-1} corresponds to characteristic vibrations of C–O bonds from alcohols (R–OH) and ethers (R–O–R), which come from the C–O stretch characteristic of cell wall carbohydrates (alginates in the case of *sargassum* and polysaccharides in the case of agro-industrial sources)

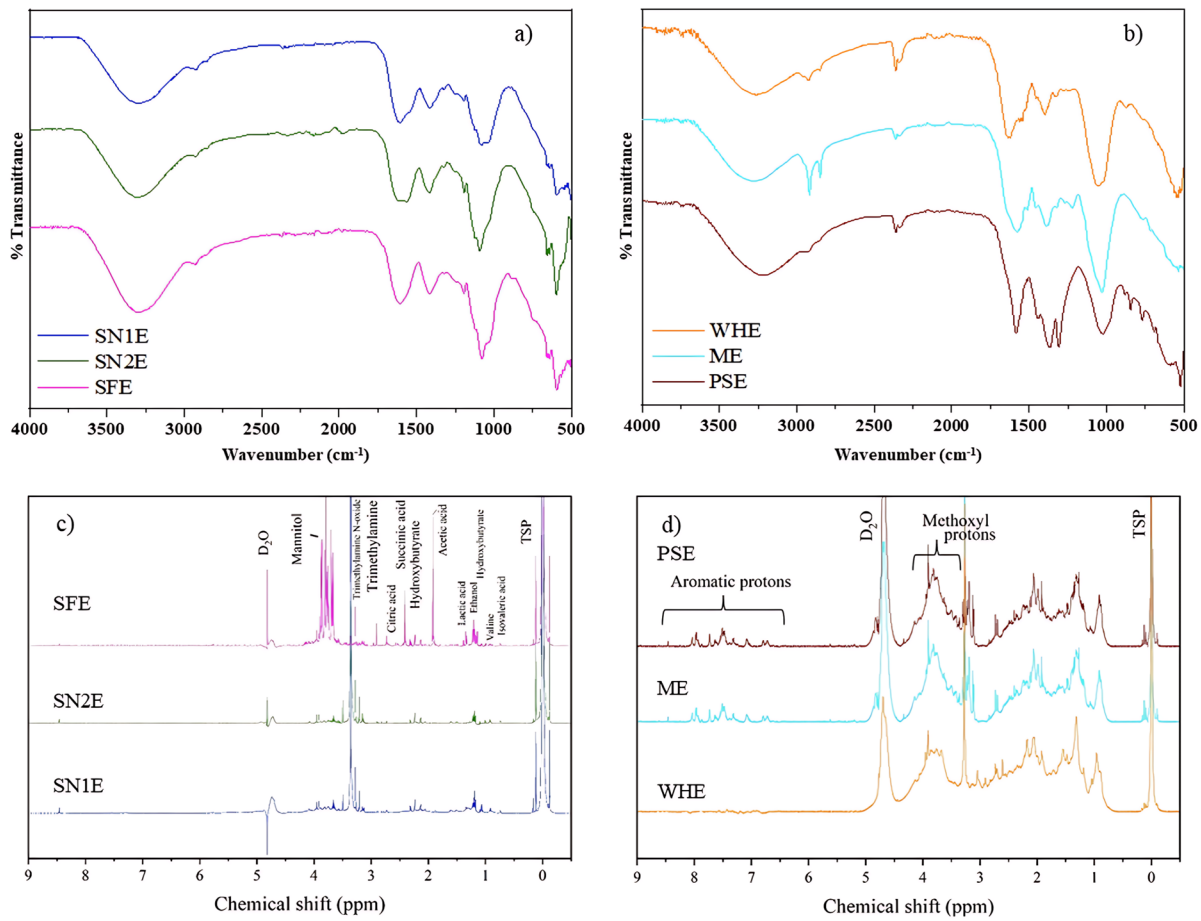

Fig. 4 FTIR and ^{1}H-NMR (in D_2O) spectra of the bio-admixtures. **a**, **c** show the spectra for *Sargassum* species, while **b**, **d** correspond to water hyacinth, miscanthus, and plantain stem extracts, respectively

[32, 33]. Noteworthy are the absorptions at 1307 (aliphatic CH_2 deformation), 1372 (aromatic methoxyl), 1445, and to a less degree, 1508 cm^{-1} (aromatic C=C vibration), being present mainly in the PSE and ME (Fig. 4b), although less intense, and which could be attributable to lignins [34–36]. This could be confirmed through ^{1}H-NMR analysis (Fig. 4d), where signals ranging from 8.00 to 6.00 ppm show similar patterns to those aromatic protons from hydroxyphenyl (7.50–7.30 ppm), guaiacyl (7.30–6.82 ppm), and syringyl units (6.82–6.30 ppm). In addition, abundant methoxyl protons were detected between 4.00 and 3.50 ppm [36]. These signals were also identified in minor concentration in WHE. In addition, several resonances around 3.00–4.00 ppm characteristic of carbinolic protons which could be attributed to sugars or polysaccharides. Meanwhile, according to their chemical shift and coupling pattern, some resonances from *sargassum* extracts (Fig. 4c) were assigned to some amino acids, fatty and organic acids [37].

3.2 Yield stress

Distinct patterns are observed in the yield stress of mortars with 0.1% and 1% bio-admixture additions. The yield stress in all mortar samples increases progressively over time (Fig. 5). For the 0.1% admixture dosage**,** REF (reference) maintained relatively higher initial yield stresses, starting at 8.10 kPa and reaching a peak of 25.47 kPa at 60 min. All mixtures containing admixtures exhibited lower initial yield stress values, indicating a liquefying effect initially. The reduction and increase of the yield stress were different for every admixture modification. SN1E and SN2E exhibited comparable development rates but slightly lower initial values than REF, with SN2E showing a pronounced increase by 60 min to 27.21 kPa, the highest among all admixtures. ME had the lowest initial yield stress at 3.36 kPa but showed a steady increase, reaching 21.66 kPa by the final time interval, highlighting a delayed but steady thickening effect.

With the 1% admixture dosage, all admixtures initially reduced the yield stress, but the time-dependent effects were more distinct than at the lower dosage. SN1E and PSE showed the most pronounced increases, with SN1E rising from 4.61 kPa at 0 min to 29.72 kPa at 60 min and PSE increasing from 2.88 kPa to 31.45 kPa. In contrast, WHE and ME exhibited relatively lower yield stress values throughout, with WHE remaining below 14 kPa across all time intervals, suggesting only a modest structural buildup. PCE at 1% dosage displayed higher initial yield stress (7.53 kPa) than at 0.1%, increasing steadily to 22.66 kPa by 60 min, indicating progressive structural buildup over time compared to the bio-admixtures. This increase in yield stress reflects structuration of the system and does not necessarily imply a corresponding change in viscosity, which was not measured in this study. Overall, increasing the

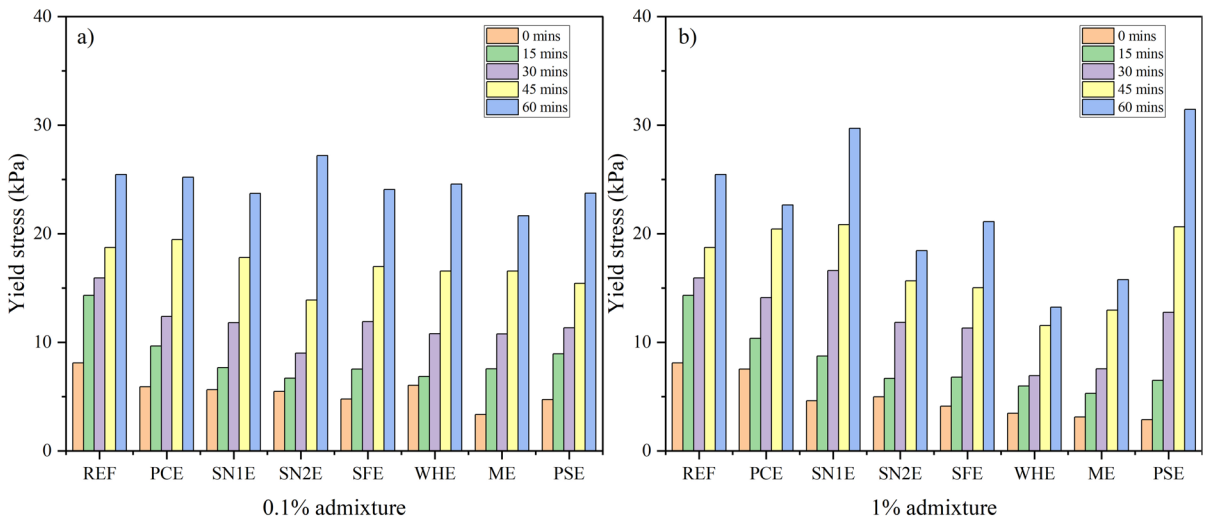

Fig. 5 Yield stress of mortars with **a** 0.1 wt% and **b** 1 wt% of admixtures

bio-admixture dosage to 1% generally enhanced the yield stress for most samples, with SN1E and PSE showing particularly substantial increases.

When comparing the efficiency of 0.1% and 1% admixture dosages, the 1% dosage generally showed a more pronounced increase in yield stress over time, reflecting a greater structural buildup in the fresh mortar. This was particularly evident for SN1E and PSE, where the higher dosage substantially increased yield stress levels at later time points (e.g., SN1E reaching 29.72 kPa and PSE peaking at 31.45 kPa by 60 min) compared to their respective performances at 0.1%.

3.3 Compressive strength

The compressive strength of mortars containing bio-admixtures at both 0.1% and 1% dosages is presented in Fig. 6. At a dosage of 0.1%, the bio-admixtures showed competitive or slightly enhanced performance compared to the reference (REF), with no significant loss in strength. After 7 days, both SN2E and SFE demonstrated improved performance, achieving strengths of 30.1 MPa and 30.2 MPa, respectively, reflecting an approximate 6% increase over REF (28.36 MPa). By 28 days, SN1E emerged as the best-performing bio-admixture, recording a 5% higher strength than REF (38.8 MPa vs. 37.06 MPa). In contrast, SFE experienced a notable decline in performance at 28 days, with its strength reducing by 15% (31.45 MPa) compared to REF. WHE, ME, and PSE exhibited moderate increases in compressive strength between 7 and 28 days, with values ranging from 34.1 MPa to 34.8 MPa at 28 days, representing 7% to 8% improvements relative to their 7-day results.

At a 1% dosage, the performance became more complex, with notable reductions in compressive strength for some bio-admixtures. After 7 days, significant decreases were observed in ME and PSE, with ME showing the most pronounced reduction—a 36% drop compared to REF (18.0 MPa vs. 28.36 MPa). PSE also experienced a 16% decrease in strength (23.9 MPa vs. REF). By 28 days, ME remained the weakest performer, recording 25.5 MPa, a 31% reduction compared to REF. Similarly, PCE showed a persistent reduction in strength, with its 28-day strength being 10% lower than REF. Conversely, SN1E continued to perform well even at the higher dosage, achieving a compressive strength of 36.9 MPa at 28 days, only 1% below REF.

3.4 Calorimetry

The rate of heat of evolution regarding the effect of the admixtures on OPC cement is shown in Figs. 6 and 7. For the REF, the onset of the acceleration period (TA) was recorded at approximately 2.24 h (Fig. 7, Table 2). The 0.1% PCE, delayed the onset of acceleration to 3.53 h, indicating a typical retardation effect. The bio-admixtures showed varied

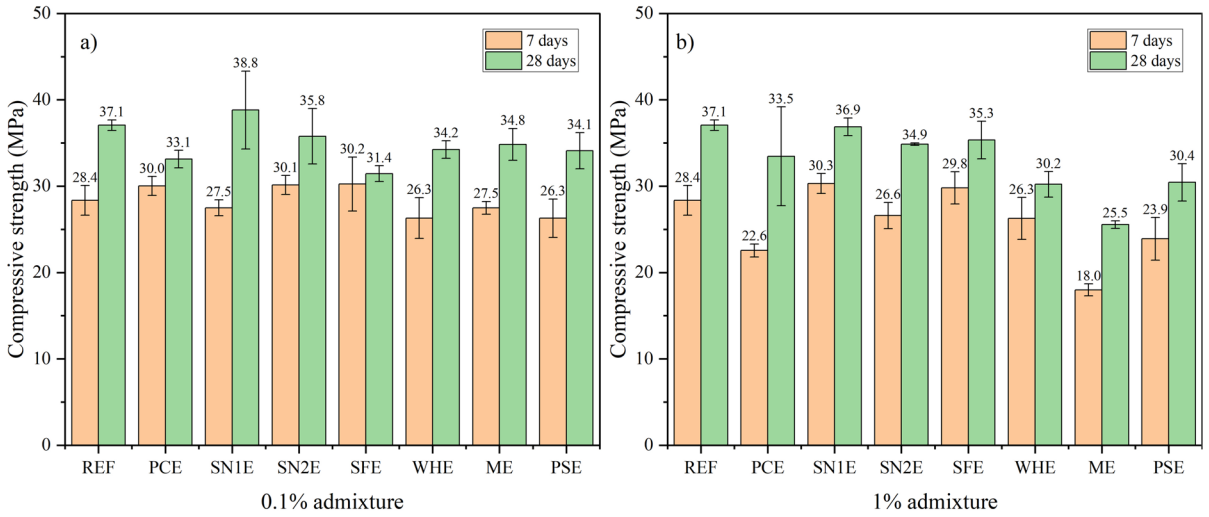

Fig. 6 Compressive strength of mortars with different dosages of admixtures

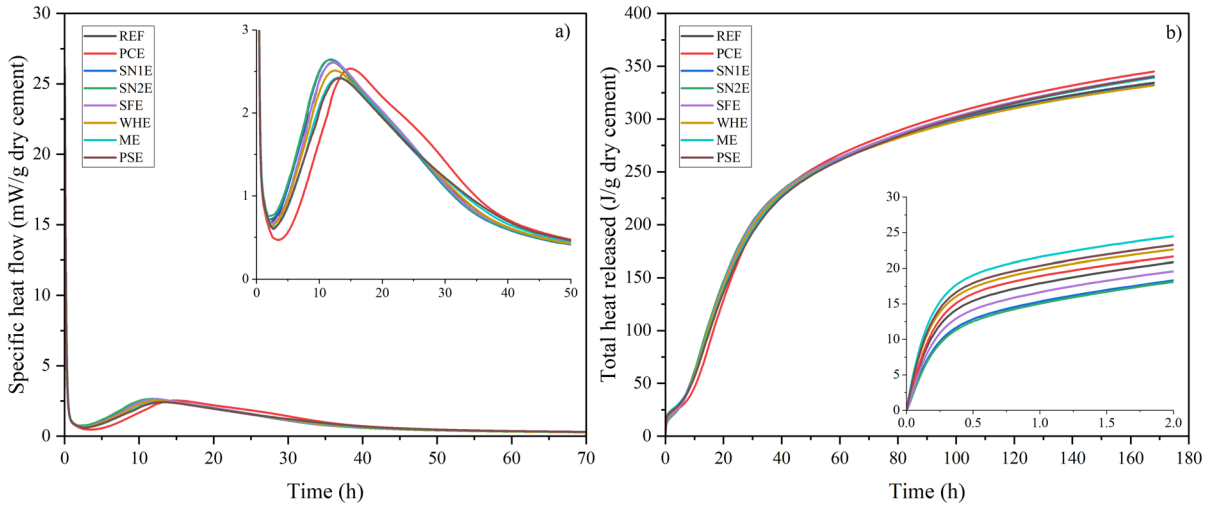

Fig. 7 **a** Specific heat flow and **b** total heat released from cement paste with 0.1% bio-admixture

Table 2 Isothermal conduction calorimetry parameters for mortar with 0.1% additive

Parameter	REF	PCE	SN1E	SN2E	SFE	WHE	ME	PSE
TA (h)[a]	2.24	3.53	2.10	2.01	2.36	2.30	2.49	2.68
Tp (h)[b]	11.99	14.87	11.68	11.67	12.11	12.39	13.08	13.26
Hp (mW/g)[c]	2.61	2.53	2.65	2.64	2.61	2.51	2.43	2.42
THp at 168 h (J/g)[d]	334.38	344.37	332.45	339.33	340.59	331.82	339.18	340.12

[a]TA: Onset of acceleration period

[b]Tp: Calorimetric peak time

[c]Hp: Peak heat flow

[d]THp: Total heat released

influence on TA: SN1E (2.10 h), SN2E (2.01 h), and SFE (2.36 h), resulting in minor changes compared to REF, while ME (2.49 h) and PSE (2.68 h) showed slight delays with 0.1% additive. Peak times (Tp) followed a similar trend, with PCE significantly delaying the hydration peak to 14.87 h, compared to 11.99 h for REF. The bio-admixtures ranged from 11.67 h for SN2E to 13.26 h for PSE. The heat released at the peak time (Hp) was relatively consistent across all samples, with values closely aligning with the REF (2.61 mW/g). Slightly higher peak heat flow was observed for SN1E, SN2E, and SFE (2.64–2.65 mW/g), while WHE, ME, and PSE showed slightly lower values (2.42–2.51 mW/g). Regarding total heat release (THp) at 168 h, all bio-admixtures showed results comparable to the REF (334.38 J/g), with PCE recording the highest value (344.37 J/g), followed closely by SFE (340.59 J/g).

The interaction between the 1% bio-admixtures and cement during early hydration extended the induction period compared to the reference sample (Fig. 8). During the acceleration phase, sargassum admixtures (SN1E, SN2E, and SFE) and WHE increased the heat flux relative to the REF, indicating that these admixtures accelerated the hydration rate. In contrast, PSE, ME, and PCE substantially reduced the maximum heat flux during this phase, highlighting their role in slowing down hydration. Among the bio-admixtures SN1E, SN2E, SFE and WHE shifted the hydration peaks to earlier times, indicating faster hydration. Conversely, ME and PSE delayed these peaks, suggesting slower hydration. The reference

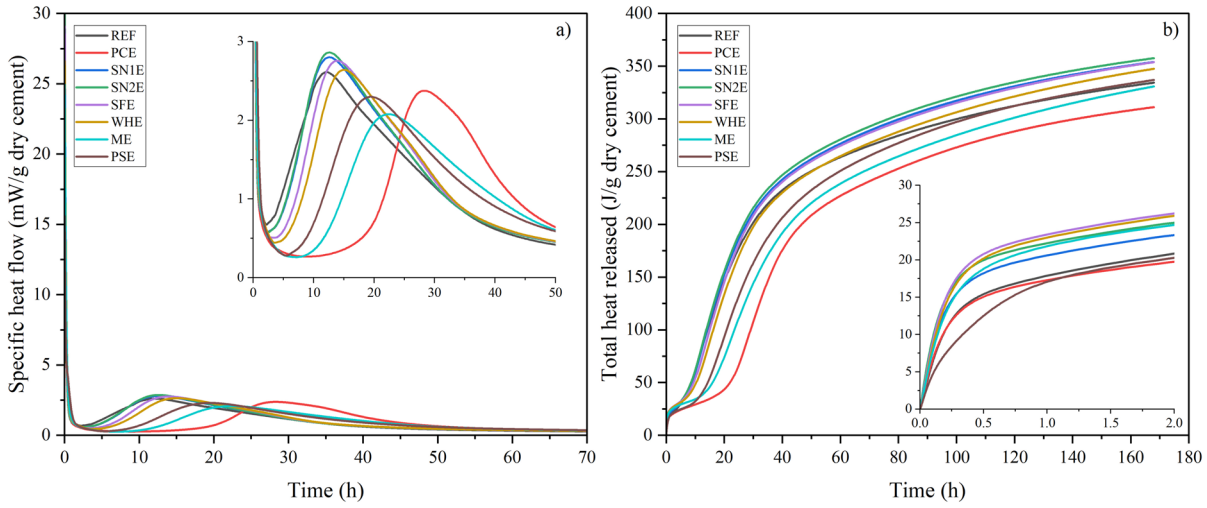

Fig. 8 **a** Specific heat flow and **b** total heat released from cement paste with 1% bio-admixture

sample exhibited a hydration peak earlier than all others, with PCE having the latest peak, confirming its pronounced retarding effect on hydration.

Table 3 shows the isothermal calorimetry results for cement paste with 1% bio-admixture. The most significant impact was observed with PCE, which delayed TA to 9.71 h, demonstrating a strong retardation effect. The bio-admixtures had a lesser but noticeable impact, with TA values ranging from 2.41 h (SN1E) to 7.26 h (ME). PCE also caused a significant delay in peak time (Tp) to 28.21 h, while the bio-admixtures had peak times ranging from 12.50 h (SN1E) to 22.18 h (ME). The peak heat flow (Hp) for bio-admixtures was generally higher than REF (2.61 mW/g), with SN1E (2.80 mW/g) and SN2E (2.86 mW/g) showing the highest values. PCE, on the other hand, had the lowest Hp at 2.37 mW/g, reflecting the retardation of hydration. In terms of total heat released at 168 h (THp), SN2E (357.57 J/g) and SN1E (353.96 J/g) outperformed the REF (334.38 J/g), while PCE recorded the lowest THp (311.09 J/g), indicating a prolonged hydration process.

3.5 TGA

The TGA and DTG of the cement paste with 1% admixture after 7 and 28 days are shown in Figs. 9 and 10, respectively. The TGA results for cement pastes with 1% bio-admixtures showed noticeable differences in weight loss within the 40–105 °C range. This range corresponds to the evaporation of free water, which is indicative of the extent of water retention and the progress of early hydration reactions. These differences highlight the varying impacts

Table 3 Isothermal conduction calorimetry parameters for cement paste with 1% additive

Parameter	REF	PCE	SN1E	SN2E	SFE	WHE	ME	PSE
TA (h)[a]	2.24	9.71	2.41	2.52	3.65	3.74	7.26	5.53
Tp (h)[b]	11.99	28.21	12.50	12.52	13.82	14.99	22.18	19.28
Hp (mW/g)[c]	2.61	2.37	2.80	2.86	2.75	2.64	2.08	2.30
THp at 168 h (J/g)[d]	334.38	311.09	353.96	357.57	353.80	347.52	330.87	337.00

[a]TA: Onset of acceleration period

[b]Tp: Calorimetric peak time

[c]Hp: Peak heat flow

[d]THp: Total heat released

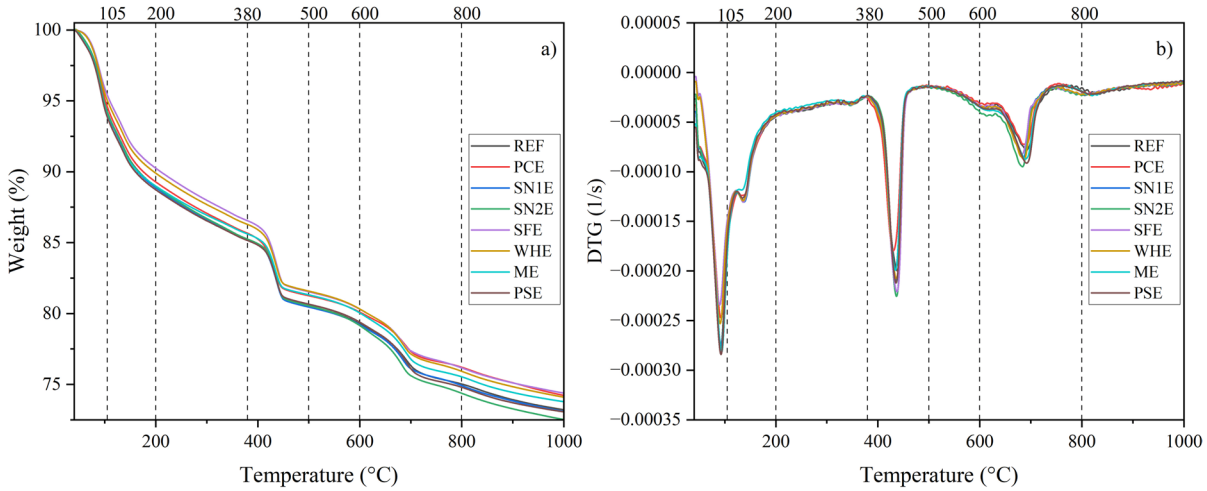

Fig. 9 TGA and DTG of cement paste with 1% bio-admixture after 7 days of hydration

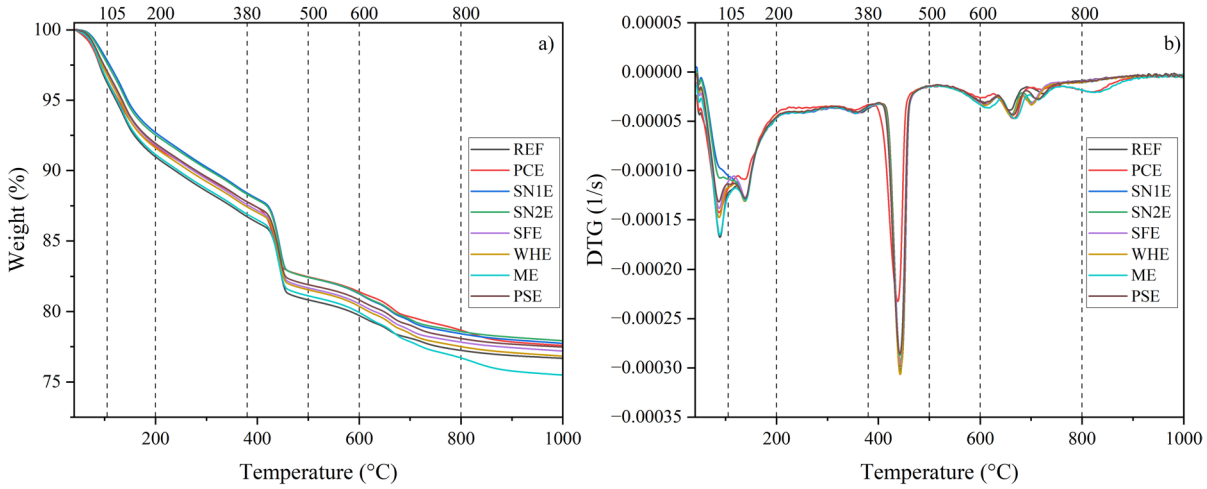

Fig. 10 TGA and DTG of cement paste with 1% bio-admixture after 28 days of hydration

of the bio-admixtures on the hydration process during the initial stages. The paste with bio-admixtures SN1E and SN2E exhibited slightly higher free water contents at 7 days, with weight losses of 5.84% and 6.01%, respectively, compared to 5.83% for the REF. This occurred despite the higher onset of acceleration and sharper calorimetric peaks observed in the isothermal calorimetry tests, indicating that these admixtures enhanced hydration primarily during the first hours. However, by 7 days their hydration degree was slightly lower than that of the reference. At 28 days, the weight losses in this range were consistently reduced for all samples, with SN1E and SN2E showing comparatively lower free water contents, which evidences a greater hydration progress over time, in agreement with the compressive strength results (Fig. 6).

In the 200–400 °C range, attributed to the decomposition of calcium silicate hydrate (C-S-H) gel, weight losses for SN1E and SN2E remained slightly elevated at 7 days (3.59% and 3.76%) compared to the REF (3.75%), signaling that these bio-admixtures support an enhanced formation of hydration products during early stages (Table 4). By 28 days, SN1E and SN2E demonstrated similar or slightly lower weight loss values than the REF in this range, suggesting that

Table 4 Weight loss associated with TG bands for cement paste with 1% bio-admixture after 7 days of hydration

Samples	% Weight loss at specific temperature (°C)						Total
	40–105	105–200	200–380	380–500	500–600	600–800	
REF	5.83	5.28	3.75	4.66	1.33	4.17	25.02
PCE	5.41	5.28	3.74	4.35	1.16	3.85	23.79
SN1E	5.84	5.33	3.59	4.81	1.17	4.37	25.11
SN2E	6.01	5.06	3.76	4.66	1.34	4.80	25.85
SFE	4.65	5.12	3.70	4.97	1.31	4.09	23.84
WHE	4.95	5.16	3.61	4.67	1.26	4.43	24.08
ME	6.04	5.03	3.37	4.27	1.29	4.46	24.46
PSE	6.16	5.18	3.52	4.47	1.27	4.62	25.22

the hydration activity associated with these admixtures stabilizes as hydration proceeds (Table 5).

The weight loss observed between 380 and 500 °C can be considered to represent the decomposition of portlandite (CH) as seen in Figs. 9 and 10. The CH content, determined by TGA, is shown in Fig. 11 for cement paste with different admixtures at both 7 and 28 days. The CH content provided additional insights into the admixtures' impact on hydration. Overall, the CH content in all paste samples increases as cement hydration progresses over time (Fig. 11). Additionally, the differences in CH content between the samples become less pronounced at later ages, suggesting that the influence of the admixtures is more significant during the early stages of hydration but diminishes as hydration continues. At 7 days, SFE (20.43%) and SN1E (19.77%) showed higher CH content than the REF (19.16%), indicating an early enhancement in calcium hydroxide formation. By 28 days, SN1E continued to display the highest Portlandite content at 24.50%, surpassing the REF (24.17%), suggesting sustained hydration over time. ME and PSE, however, showed Portlandite contents closer to the REF by 28 days (23.76% and 24.21%, respectively), indicating that their hydration rates are more moderate compared to SN1E and SN2E.

In terms of total weight loss, the REF, SN1E, SN2E, and PSE exhibited relatively stable hydration profiles at both time points, maintaining approximately 25% total weight loss at 7 days and 22% by 28 days. PCE, on the other hand, showed the lowest total weight loss across both time points, with 23.79% at 7 days and a further reduced 21.43% at 28 days. This supports the understanding that PCE's strong retardation effect reduces the overall hydration rate, contrasting with the accelerating effects of the bio-admixtures.

In summary, the TGA data suggest that SN1E, SN2E, and SFE are retard less the early hydration and promoting calcium hydroxide formation, evidenced by their higher weight losses and elevated Portlandite (CH) contents at 7 days. ME and PSE exhibit a delayed but steady hydration process, indicating a less pronounced effect on hydration rates. PCE consistently reduces hydration activity, demonstrating the most substantial retardation effect among the

Table 5 Weight loss associated with TG bands for cement paste with 1% bio-admixture after 28 days of hydration

Samples	% Weight loss at specific temperature (°C)						Total
	40–105	105–200	200–380	380–500	500–600	600–800	
REF	3.72	5.35	4.27	5.88	1.15	2.34	22.71
PCE	3.62	4.66	3.92	5.34	1.04	2.85	21.43
SN1E	2.26	5.13	4.35	5.96	1.17	2.79	21.66
SN2E	2.48	5.08	4.24	5.85	1.10	2.68	21.43
SFE	3.12	5.12	4.30	5.88	1.05	2.78	22.25
WHE	3.27	5.17	4.21	5.86	1.21	2.85	22.57
ME	3.58	5.30	4.23	5.78	1.27	3.08	23.24
PSE	3.05	5.03	4.14	5.89	1.23	2.58	21.92

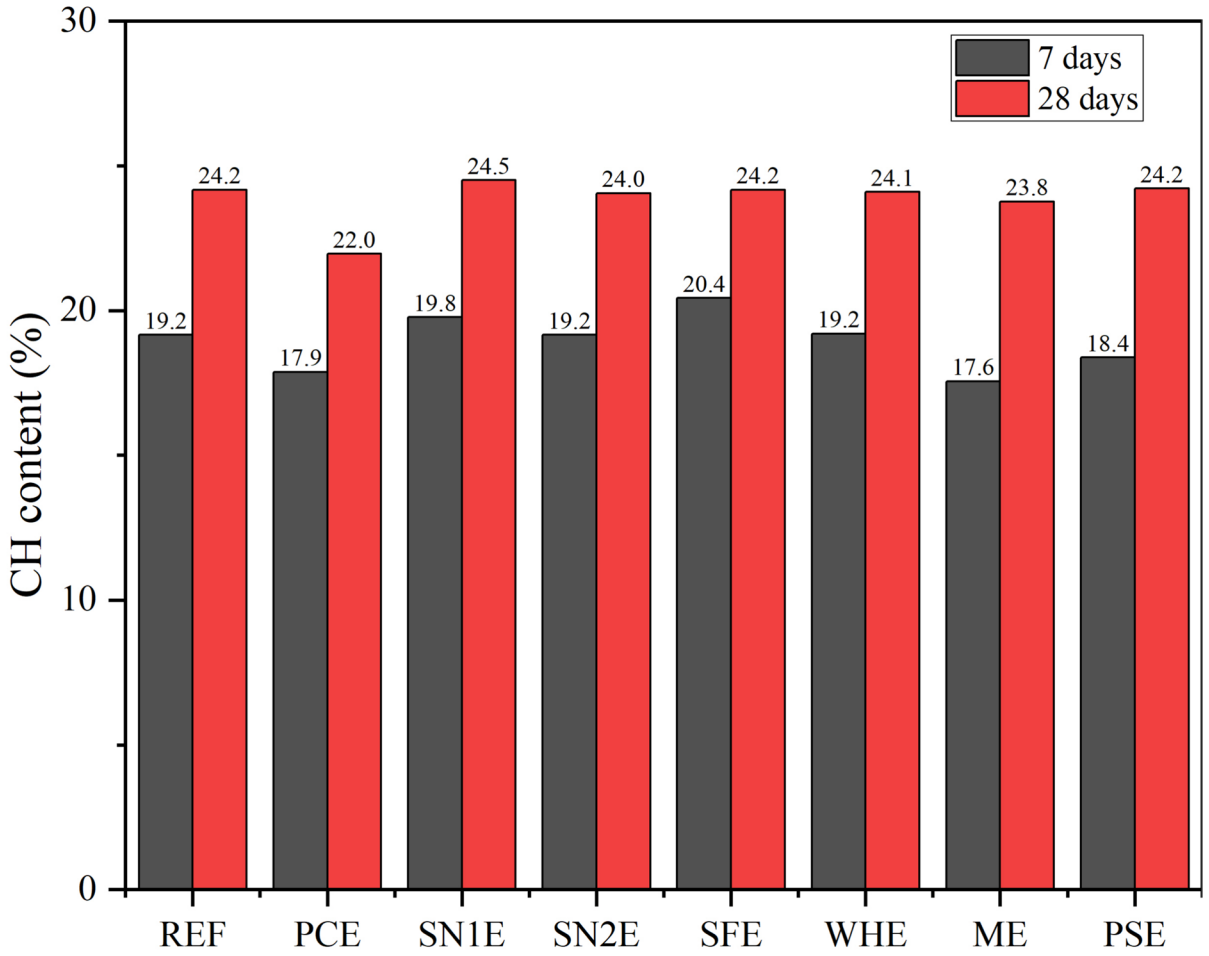

Fig. 11 Effect of admixture type on the portlandite (CH) content

admixtures, as seen by its lower total weight loss and reduced CH content across both time points.

3.6 XRD

The XRD patterns of the hydrated pastes after 7 days and 28 days of curing containing 1% of bio-admixture are shown in Fig. 12. For all pastes, typical reflections of the anhydrous phases of Portland cement, alite (C_3S), and belite (C_2S) were observed, along with hydrated phases such as ettringite, portlandite (CH), and the AFm phase of hemicarbonate. The C-S-H gel was identified through the amorphous halo between 25 and 35° 2θ and the characteristic peak at 29°, the latter of which could also be associated with calcite formation.

At 7 days of hydration, monocarbonate was identified only in the PCE sample. However, at 28 days, monocarbonate was detected in the REF, PCE, ME, and PSE samples. A reduction in the intensity of the anhydrous phase reflections was observed from 7 to 28 days of hydration, along with an increase in the intensity of the peak at 29°. The ME sample exhibited the smallest reduction in anhydrous phase peaks between 7 and 28 days. Regarding portlandite, an increase in peak intensity was noted, decreasing in magnitude across the samples in the following order: PCE, ME, PSE, SFE, WHE, SN1E, SN2E, and REF.

Figure 14 presents a zoomed-in view of the 2θ between 10° and 25°, highlighting peaks associated with the presence of whewellite ($CaC_2O_4{\cdot}H_2O$) after 7 days of hydration in the ME and PSE samples. Notably, at 28 days, the intensity of the

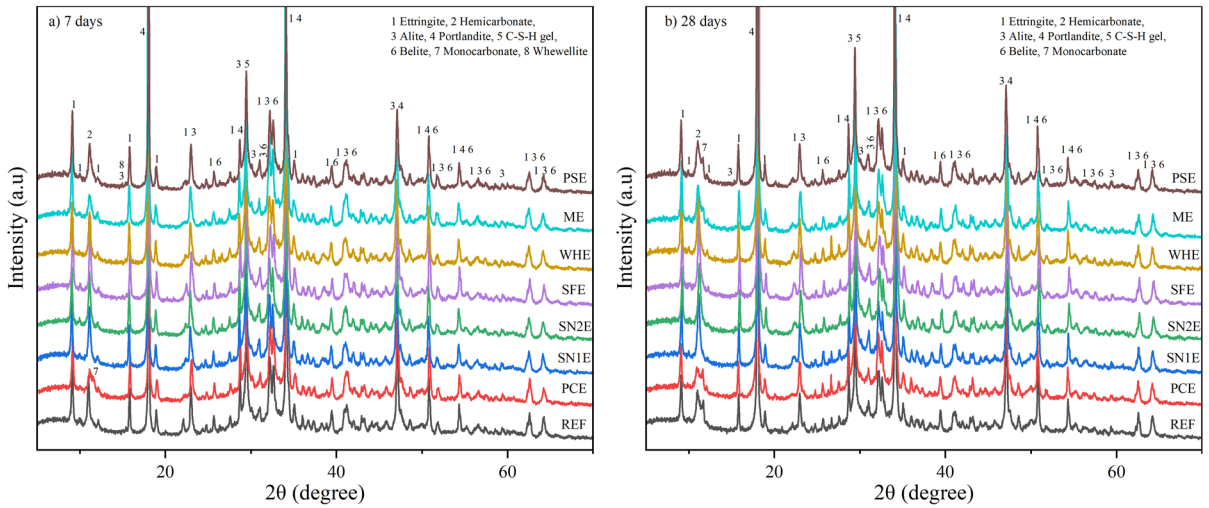

Fig. 12 XRD patterns of the pastes after **a** 7 days and **b** 28 days of curing

whewellite-associated peaks decreases, coinciding with the formation of a monocarbonate phase.

4 Discussion

This study evaluates bio-based admixtures derived from agricultural sources (PSE—plantain stem extract and ME—miscanthus extract) and aquacultural sources (*Sargassum natans* N I (SN1E), *Sargassum natans* N VIII (SN2E), *Sargassum fluitans* (SFE), and water hyacinth (WHE)). The objective was to assess their influence on the yield stress of cementitious systems to determine their potential as plasticizers and their effects on the hydration process of Portland cement and the compressive strength of cement-based materials.

4.1 Yield stress and hydration

The yield stress results (Fig. 5) showed that all bio-admixtures reduced yield stress compared to the reference (REF), indicating their ability to enhance workability. At a 1% dosage, PCE exhibited the greatest reduction in yield stress after one hour. However, PCE at 1% dosage displayed a higher initial yield stress (7.53 kPa) than at 0.1%, increasing to 22.66 kPa by 60 min. This increase may be linked to overdosing effects, where excess PCE leads to segregation and changes in particle packing, causing the trigger load to appear at deeper penetration levels. Similar observations have been reported when PCE superplasticizers exceed their optimal dosage range [38, 39]. Beyond surface saturation, non-adsorbed PCE molecules remain in the pore solution and can induce depletion forces, promoting particle flocculation and a rise in yield stress [40, 41]. At a 1% dosage, SN2E, SFE, WHE, and ME exhibited a reduction in yield stress after one hour. In contrast, SN1E and PSE increased yield stress at all evaluated time intervals, suggesting a structuring effect. Notably, WHE and ME maintained relatively low yield stress values, indicating a milder thickening influence that could favor extended workability. Overall, the 1% bio-admixture dosage produced greater thickening effects in most cases, enhancing early-age rigidity, whereas the 0.1% dosage resulted in a more gradual increase in yield stress. These findings suggest that WHE, ME, and PSE are more effective at prolonging workability, while bio-admixtures derived from sargassums tend to reduce workability.

Calorimetry results (Fig. 8) revealed that bio-admixtures generally slowed the hydration reaction but not to the extent observed with PCE. Among all tested admixtures, PCE exhibited the most extended delay in the onset of the acceleration phase, highlighting its strong retarding effect. In contrast, the biopolymers retarded hydration to a lesser extent while still providing workability improvements, at least in terms of static yield stress (Fig. 5).

The influence of organic molecules on cement hydration kinetics can be broadly classified into two mechanisms: (1) direct interactions with inorganic surfaces, including unhydrated cement particles and hydration products, and (2) indirect interactions with the pore solution, altering the hydration environment. Upon entering the liquid phase, these interactions begin immediately and persist for a certain duration, referred to as the "action time". This action time depends on molecular properties and the availability of free molecules [42]. For bio-admixtures, used in this study, the action time is relatively short (i.e., as retardation effect was shorter), primarily affecting early hydration stages. During this period, the initial C-S-H nuclei form but do not grow extensively [42]. Free molecules in the solution inhibit the nucleation and growth of C-S-H, leading to temporary retardation of hydration. Once these molecules are depleted, hydration resumes at a normal rate, resulting in the main hydration peak [43, 44].

Incorporating bio-admixtures introduces complex interactions between polymers (i.e., from the bio-admixtures) and hydration products in the solution. Polymers can adsorb onto cement particles and hydration products, slowing down dissolution and hydration (e.g. the CH content in the present study was different for each admixture added, Fig. 11). Zeta potential values measured in water were generally more negative across all samples, ranging from -9.26 mV for PCE to approximately -22 to -34 mV for the bio-based admixtures. When dispersed in $Ca(OH)_2$, the zeta potential of all polymers shifted toward less negative values due to ionic screening and Ca^{2+} interactions. For example, the zeta potential of PCE decreased from -9.26 mV in water to -5.11 mV in $Ca(OH)_2$, while the bio-admixtures showed a reduction from approximately -30 mV to -14 mV (see Table 1). This consistent reduction across all samples supports the hypothesis that these polymers adsorbed onto cement particle surfaces (although not all polymers may be adsorbed), where charge neutralization or calcium bridging occurred.

While both PCE and the bio-admixtures appear to adsorb onto cement surfaces, differences in their particle sizes suggest distinct adsorption behaviors and implications for hydration. PCE had a small size (~ 65 nm in water and ~ 172 nm in $Ca(OH)_2$), allowing it to form a relatively continuous, compact adsorption layer on cement particles (i.e., even coverage). This likely limits the available surface area for hydration reactions and inhibits the growth of hydration products in multiple directions, thereby contributing to its well-known retardation effects. In contrast, the bio-admixtures presented larger and more variable particle sizes, ranging from ~ 110 to ~ 200 nm in water and from ~ 155 to ~ 410 nm in $Ca(OH)_2$. Their bulkier, less uniform structures, while still adsorbing onto cement particles, may not form an equally dense or uniform coverage (i.e., uneven or patchier coverage). As a result, these biopolymers may partially block the surface but still allow for continued nucleation and growth of hydration products in several directions. This structural difference may explain the observed less pronounced retardation effects (Figs. 7a and 8a) in the biopolymer-containing systems compared to PCE. A conceptual model was developed in connection with the hypothesis on polymer adsorption and cement hydration behavior, illustrated in a schematic in Fig. 13.

In addition to physical adsorption behavior, the authors believe that the presence of dissolved inorganic ions in the bio-admixtures, as identified in the XRD analysis, may also contribute to the hydration process. These ions -potentially including chlorides, potassium, and sodium- can influence the ionic environment of the pore solution and may interact with cement hydration kinetics, either by accelerating or moderating early-stage reactions. Although their precise role is discussed in later sections, it is proposed here that these dissolved ions may have overlapping or competing effects with polymer adsorption. Combined with the looser surface coverage provided by the larger bio-based polymers, this dual influence may help explain the reduced hydration retardation and increase the yield stress (reduced workability) observed in bio-admixture systems when compared to the PCE.

4.2 Influence of aquaculture bio-admixtures (SN1E, SN2E, SFE and WHE) on hydration and strength

At a lower dosage, SN1E and SN2E promoted early hydration, as indicated by an increase in C-S-H formation and a slightly higher total heat release compared to the reference. This suggests that the admixtures enhanced the degree of hydration, likely by modifying the ionic composition of the pore solution and increasing calcium silicate phase dissolution. The

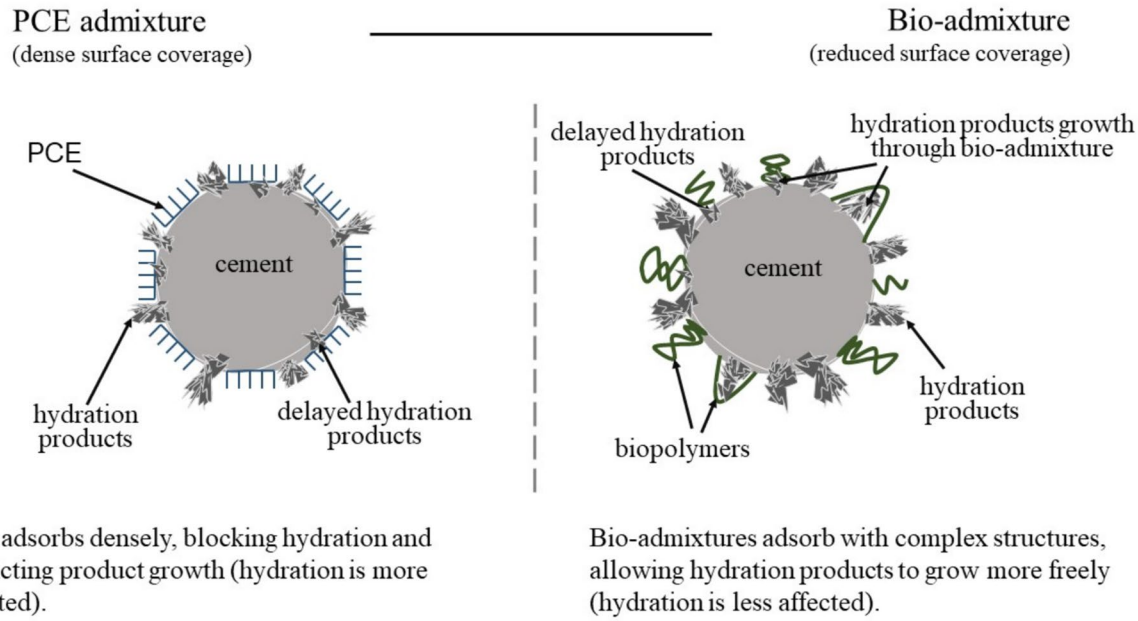

Fig. 13 Schematic illustration of admixture adsorption and its influence on cement hydration product growth for PCE and bio-based admixtures

presence of chloride ions in these admixtures may have weakened the protective layer of early hydration products, leading to a faster transition into the acceleration phase [45]. However, no formation of Friedel's salt was detected, suggesting that the interaction between chloride and C_3A was limited. NaCl dosages up to 5 wt% have been reported to shorten the induction period of calcium silicate phases, accelerating the transition to the main hydration phase of C_3S and increasing the associated heat flow [46]. Similarly, KCl is known to slightly delay the setting time of ordinary Portland cement. However, in oil well cementing, NaCl has a dual effect: it accelerates hydration at lower dosages but retards it when used in higher concentrations [47]. A comparable behavior was observed with the sargassum-based bio-admixtures (SN1E, SN2E, and SFE), likely due to their significant content of sylvite (KCl) and halite (NaCl), as confirmed by XRD analysis (Fig. 1).

In comparison to the sargassum-based admixtures, WHE exhibited a slightly prolonged induction period and a lower peak height, indicating a milder retarding effect. Although XRD analysis confirmed the presence of KCl and NaCl in WHE (Fig. 1), their peak intensities were lower than those observed for the sargassum admixtures. This suggests that while WHE influenced hydration in a similar manner to sargassum admixtures, it did so to a lesser extent, leading to a slightly longer retardation effect.

The trends observed in compressive strength development at 7 and 28 days align well with the findings from thermal analysis (TGA/DTG) and calorimetry. Portlandite (CH) content, inferred from TGA results, served as an indicator of hydration progress. Mortars incorporating sargassum-based bio-admixtures (SN1E, SN2E, and SFE) exhibited higher CH content in the 380–500 °C range, suggesting more active hydration at early stages. This corresponded to their relatively higher early strengths at 7 days.

Comparing 0.1% and 1% dosages, SN1E and SN2E demonstrated relatively stable strength gains. At 0.1%, SN1E showed a 5% higher 28-day strength than the reference, while at 1%, the strength remained nearly unchanged, decreasing by only 1%. Similarly, SN2E maintained 97% of the reference strength at 0.1% dosage but experienced a 6% drop at 1%, indicating a slight delay in hydration at the higher dosage. Despite this, the retardation was not as severe as observed with other admixtures.

4.3 Influence of agricultural-based bio-admixtures (PSE and ME) on hydration and strength

In contrast to other bio-admixtures, those derived from plantain stem (PSE) and miscanthus (ME) exhibited a more pronounced retarding effect on cement hydration, particularly at the 1% dosage. The extended induction period and delayed acceleration phase observed in calorimetric analysis suggest that these admixtures interfered significantly with early-stage hydration, resulting in lower cumulative heat release and a broader, less-defined hydration peak. This behavior is likely attributed to differences in their chemical composition, particularly the presence of potassium oxalate hydrate ($K_2C_2O_4{\cdot}H_2O$) in PSE, and potassium bicarbonate and weddellite ($CaC_2O_4{\cdot}2H_2O$, calcium oxalate) in ME.

The interaction of oxalate ions with calcium ions (Ca^{2+}) released from early hydration phases (C_3S and C_3A) may have led to the formation of insoluble calcium oxalate (CaC_2O_4), thereby reducing the availability of free Ca^{2+} needed for continued hydration [48]. This phenomenon was confirmed by XRD analysis after 7 days of hydration (Fig. 14). Additionally, the precipitation of calcium oxalate could have formed a protective layer around cement particles, delaying dissolution and subsequently slowing the hydration reactions. This effect was particularly noticeable in PSE mortars, which showed longer hydration peak times in calorimetry and reduced early-age strength.

The ME admixture, containing both oxalate and bicarbonate species, likely exhibited a combined influence on cement hydration. While the role of oxalate has already been discussed, the presence of potassium bicarbonate may have further delayed hydration by competing with sulfate ions. This competition favored the formation of hemicarbonates or monocarbonates at the expense of ettringite formation (Fig. 14). As demonstrated by Kunther et al. [49], high bicarbonate concentrations destabilize both ettringite and gypsum, disrupting the sulfate balance and altering the normal sequence of hydration phase development. Such disruption likely contributed to the prolonged setting times and lower early compressive strengths observed in ME-modified mortars.

Although the bio-admixtures contained dissolved ions, the authors propose that the primary mechanism influencing hydration behavior was the adsorption of bio-admixture molecules onto the cement particle surfaces. The dissolved ions present in the admixtures likely exerted an additional, overlapping influence on hydration retardation, but their impact appears to be secondary compared to the adsorption mechanism. At 0.1% dosage, the retardation effect was less pronounced, likely due to the rapid depletion of free molecules in the solution. Once these molecules were adsorbed or reacted, hydration kinetics resumed along a normal path. However, at 1% dosage, the persistence of free molecules in solution continued to interfere with hydration processes, leading to significantly lower early strengths. This was particularly evident for ME, which showed a 27% reduction in compressive strength when the dosage increased from 0.1 to 1%.

An additional feature that could influence the behavior of hydration processes is the presence of certain groups of molecules in PSE and ME bio-admixtures. According to FTIR and ^{1}H-NMR spectra, these biomaterials may contain traces of lignins, which are natural polymers constituting the cell wall of plants and are formed by phenylpropanoids such as guaiacyl, syringyl, and hydroxyphenyl units. The presence of these phenolic groups could be related to the delay in cement hydration, since they were detected in higher concentration in PSE and ME, as observed in the aromatic region of ^{1}H-NMR spectra. Other polyphenols from the bark of the *Albizia tomentosa* tree have shown to gradually improve the durability properties of cement mortars (electrical resistivity, ultrasonic wave propagation, and water absorption by capillarity) at curing times of 7, 28, and 96 days [50]. The authors concluded that the possible mechanism of action is through the polymerization of tannins and other polyphenols, causing an increase in molecular size, thus filling the microcracks produced during cement hydration [1].

ME and PSE pastes showed lower CH content at early ages, supporting the conclusion that hydration was significantly delayed. The increased mass loss in the 40–105 °C range in these samples indicated higher amounts of physically adsorbed water, suggesting that less bound water was integrated into C-S-H gels by 7 days. By 28 days, however, CH content in these pastes had increased substantially (35.4% and 31.7% for ME and PSE, respectively- Table 6), reflecting a more prolonged but ultimately progressive hydration process.

Recent studies have highlighted the potential of bio-based admixtures as sustainable alternatives to conventional chemical additives in cementitious systems. Ekop et al. [51] reviewed a wide range of bio-admixtures and reported their ability to enhance workability, strength, and durability. Venkatraman and Ramasamy [52] showed that gums such as gum Arabic and guar gum improved compressive strength at low dosages but caused strength reduction at higher levels, underscoring the importance of dosage optimization. Similarly, Fang et al. [53] observed that black tea extract significantly retarded cement hydration but improved mortar strength at all ages, attributing this effect to enhanced dispersion of cement particles. These findings are consistent with the present study, where the influence of agricultural- and aquacultural-derived admixtures on hydration and strength varied with dosage and composition. Together, they demonstrate a growing body of evidence that bio-based admixtures can be effective in modifying cement hydration and performance when appropriately tailored.

The findings of this study suggest that dosage optimization is critical when applying bio-admixtures in cementitious systems. At lower dosages (0.1%), all mortars showed comparable or slightly higher strength, with some improvement in workability. At higher dosages (1%), miscanthus, plantain stem, and water hyacinth admixtures caused significant strength reductions due to prolonged hydration delay, although they improved workability, while sargassum-based admixtures retained a more balanced performance with better strength preservation. From a practical perspective, this indicates that lower dosages are most suitable for general applications requiring a balance between workability and strength. Higher dosages, in contrast, may be considered only in specific cases such as 3D printing or concreting in hot climates, where extended setting times and enhanced structuration are advantageous. These results highlight the need to tailor dosage not only to the desired rheological behavior but also to the specific origin and chemical nature of the bio-admixture.

5 Summary and conclusion

The results of this study demonstrate that bio-admixtures derived from agricultural and aquacultural sources significantly influence the rheological properties (yield stress), hydration kinetics, and mechanical performance of cementitious systems. These effects varied depending on the type and dosage of the bio-admixtures. Based on the results the following conclusions were made:

- At 0.1% dosage, most bio-admixtures did not significantly alter yield stress. However, at 1% dosage, sargassum-based admixtures (SN1E, SN2E, and SFE) increased yield stress over time, indicating their ability to enhance structural buildup while providing sufficient flowability for practical applications. Water hyacinth extract (WHE) and miscanthus extract (ME) presented a milder thickening effect that extended workability. Plantain stem extract (PSE) exhibited a notable increase in yield stress over time, particularly at 1% dosage, leading to early structuration of the cement paste, beneficial for 3D printing or self-consolidating concrete.
- Bio-admixtures exhibited milder retardation effects, allowing for better early-age hydration, when compared with PCE. Sargassum-based admixtures accelerate initial hydration at 0.1% dosage, due to KCl and NaCl content, but at 1% dosage, the hydration process was slightly delayed. WHE exhibited a slightly longer induction period. ME and PSE exhibited the most pronounced retardation effects, particularly at 1% dosage.
- While bio-admixtures demonstrate promising potential for enhancing or maintaining compressive strength at lower dosages (0.1%), with SN1E and SN2E showing a notable 5% improvement, higher dosages (1%) can lead to significant strength reductions due to increased hydration retardation, particularly observed in ME and PSE. Notably, sargassum-based admixtures and WHE exhibited better strength retention at the higher dosage, with SN1E maintaining a substantial 97% of the reference strength. Therefore, careful dosage optimization of these bio-admixtures is crucial to harness their benefits without compromising strength development, especially in applications demanding high early strength.
- Thermal analysis revealed that REF, SN1E, SN2E, and PSE showed stable hydration with ~ 25% weight loss at 7 days. PCE exhibited the lowest weight loss, confirming its strong retarding effect.

SN1E, SN2E, and SFE minimally retarded early hydration and promoted CH formation, while ME and PSE showed slower, continuous hydration. PCE consistently reduced hydration activity.

Overall, bio-based admixtures show potential as eco-friendly alternatives to conventional superplasticizers, with their effects varying based on dosage, chemical composition, and interaction with cement hydration. The observed retardation effects should not be viewed as the primary objective of incorporating these bio-admixtures but rather as a side effect that can be beneficial or detrimental depending on the intended application. WHE may offer a viable alternative for extended workability. While sargassum-based admixtures and WHE exhibit promising hydration and strength properties, the optimal dosage and mix design must be carefully selected to balance rheology modification and strength development in sustainable concrete formulations. The delayed hydration observed in PSE and ME mortars may be advantageous in applications requiring extended workability, particularly in hot climates where rapid setting can be an issue. Further studies are recommended to optimize dosage levels and investigate the long-term durability of bio-admixture-modified cementitious systems. It should also be noted that the chemical composition of bio-admixtures from agricultural and aquacultural sources can vary with growth conditions, environmental factors, and processing, which may influence their performance in cementitious systems. Future work should therefore consider strategies for consistent characterization and standardization of these materials.

Acknowledgements The authors sincerely thank the Deutsche Gesellschaft für Internationale Zusammenarbeit (GIZ), Germany, Project: *From Agriculture waste to CO_2-friendly concrete* (No. 81290256), for financial support, which made this research possible. We gratefully acknowledge additional funding from the DAAD Bilateral Exchange of Academics Project: *Bio-construction Materials from Seaweed Pollution (Sargassum)* (No. 91871251). Special thanks to Dr. Patrick Cunningham for assistance with the visualization of the proposed concept. The Energy and Materials In-situ Laboratory Berlin (EMIL) operated by the Helmholtz-Zentrum für Materialien und Energie GmbH (HZB) is acknowledged for granting access to its chemistry/ sample characterization laboratory. We also thank the Laboratorio Nacional de Nano y Biomateriales (LANNBio), CINVESTAV-Mérida, for access to laboratory facilities and characterization equipment. In particular, we appreciate the support of Dr. Gloria Ivonne Hernández Bolio and Lic. Dylan Díaz for providing the *Sargassum* samples. We further acknowledge MSc. Marco Antonio Vera Ramírez and the NMR Laboratory at Universidad Autónoma Metropolitana, Unidad Iztapalapa, for conducting the ^{1}H-NMR analysis.

Author contributions Conceptualization: Bright Asante, Wolfram Schmidt; Methodology: Bright Asante, Wolfram Schmidt; Formal analysis and investigation: Bright Asante, Luís Urbano Durlo Tambara, Montserrat Soria-Castro; Writing—original draft preparation: Bright Asante; Writing—review and editing: Bright Asante, Luís Urbano Durlo Tambara, Montserrat Soria-Castro, Alejandra Ramírez, Pedro Castro Borges, Wolfram Schmidt; Funding acquisition: Wolfram Schmidt; Montserrat Soria-Castro Resources: Wolfram Schmidt, Pedro Castro Borges, Alejandra Ramírez; Supervision: Wolfram Schmidt, Pedro Castro Borges.

Funding Open Access funding enabled and organized by Projekt DEAL.

Data availability Data will be made available on request.

Appendix

See Table 6 and Fig. 14.

Table 6 Portlandite (CH) content associated with TG band between 380 and 500 °C

Sample	7 days Portlandite (%)	28 days Portlandite (%)	Diff in CH	% increase in CH content
REF	19.16	24.17	5.01	26.15
PCE	17.88	21.95	4.07	22.76
SN1E	19.77	24.50	4.73	23.93
SN2E	19.16	24.05	4.89	25.52
SFE	20.43	24.17	3.74	18.31
WHE	19.2	24.09	4.87	25.47
ME	17.55	23.76	6.21	35.38
PSE	18.38	24.21	5.83	31.72

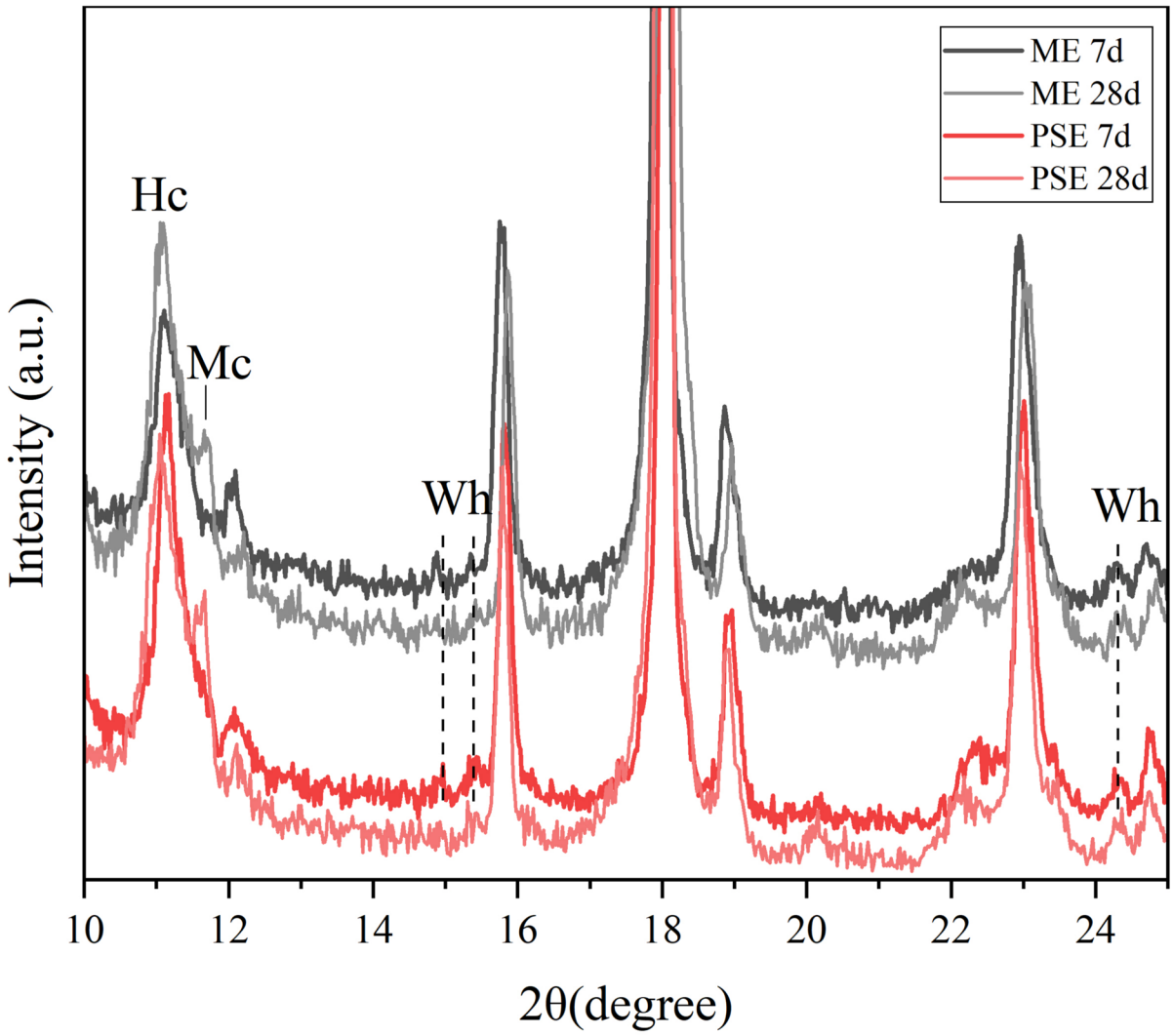

Fig. 14 XRD patterns zoom area for ME and PSE samples (Hc—hemicarbonate, Mc—monocarbonate, Wh—Whewellite)

References

1. Mahmood HF, Dabbagh H, Mohammed AA (2021) Comparative study on using chemical and natural admixtures (grape and mulberry extracts) for concrete. Case Stud Constr Mater. https://doi.org/10.1016/j.cscm.2021.e00699
2. Plank J, Hirsch C (2007) Impact of zeta potential of early cement hydration phases on superplasticizer adsorption. Cem Concr Res 37(4):537–542. https://doi.org/10.1016/j.cemconres.2007.01.007
3. Schmidt W, Brouwers HJH, Kühne H-C, Meng B (2014) Influences of superplasticizer modification and mixture composition on the performance of self-compacting concrete at varied ambient temperatures. Cem Concr Compos 49:111–126. https://doi.org/10.1016/j.cemconcomp.2013.12.004
4. Hanehara S, Yamada K (1999) Interaction between cement and chemical admixture from the point of cement hydration, absorption behaviour of admixture, and paste rheology. Cem Concr Res 29(8):1159–1165. https://doi.org/10.1016/s0008-8846(99)00004-6
5. Plank J, Winter C (2008) Competitive adsorption between superplasticizer and retarder molecules on mineral binder surface. Cem Concr Res 38(5):599–605. https://doi.org/10.1016/j.cemconres.2007.12.003
6. Flatt RJ, Houst YF (2001) A simplified view on chemical effects perturbing the action of superplasticizers. Cem Concr Res 31(8):1169–1176. https://doi.org/10.1016/s0008-8846(01)00534-8
7. Flatt RJ (2004) Dispersion forces in cement suspensions. Cem Concr Res 34(3):399–408. https://doi.org/10.1016/j.cemconres.2003.08.019

8. Yoshioka K, Tazawa E-I, Kawai K, Enohata T (2002) Adsorption characteristics of superplasticizers on cement component minerals. Cem Concr Res 32(10):1507–1513. https://doi.org/10.1016/s0008-8846(02)00782-2
9. Schmidt W, Brouwers HJH, Kuehne H-C, Meng B (2012) Influence of temperature on stabilizing agents in presence of superplasticizers. Presented at the Tenth International Conference on Superplasticizers and Other Chemical Admixtures in Concrete, Prague, Czech Republic
10. Glaus MA, Laube A, Van Loon LR (2011) A generic procedure for the assessment of the effect of concrete admixtures on the sorption of radionuclides on cement: concept and selected results. MRS Proc. https://doi.org/10.1557/proc-807-365
11. Schmidt W, Peters S, Kühne H-C (2015) Effects of particle volume fraction and size on polysaccharide stabilizing agents. In: Malhotra VM (ed) SP-302: eleventh international conference on superplasticizers and other chemical admixtures in concrete, pp 39–52. https://doi.org/10.14359/51688083
12. Khayat KH (1998) Viscosity-enhancing admixtures for cement-based materials—an overview. Cem Concr Compos 20(2–3):171–188. https://doi.org/10.1016/s0958-9465(98)80006-1
13. Rajayogan V, Santhanam M, Sarma BS (2003) Evaluation of hydroxy propyl starch as a viscosity-modifying agent for self compacting concrete. Presented at the 3rd International RILEM Symposium on Self-Compacting Concrete, Reykjavik, Iceland
14. Izumi T, Dikty S, Yamamuro H (2006) Properties of new polysaccharide as a thickener for concrete. Presented at the 8th CANMET/ACI International Conference on Superplasticizers and other chemical Admixtures in Concrete, Sorrento, Italy
15. Schmidt W, Kuehne H-C (2007) Influence of the processing temperature on the properties of SCC in the presence of superplasticizer and other admixtures. Concr Plant Precast Technol 40–49
16. Patural L, Govin A, Ruot B, Devès O, Grosseau P (2009) Influence of cellulose ether particle size on water retention of freshly mixed mortars. Presented at the Ninth ACI International Conference on Superplasticizers and Other Chemical Admixtures in Concrete, Seville, Spain
17. Peschard A, Govin A, Grosseau P, Guilhot B, Guyonnet R (2004) Effect of polysaccharides on the hydration of cement paste at early ages. Cem Concr Res 34(11):2153–2158. https://doi.org/10.1016/j.cemconres.2004.04.001
18. Abd El-Rehim HA, Hegazy E-SA, Diaa DA (2013) Radiation synthesis of eco-friendly water reducing sulfonated starch/acrylic acid hydrogel designed for cement industry. Radiat Phys Chem 85:139–146. https://doi.org/10.1016/j.radphyschem.2012.11.002
19. Afroz S, Manzur T, Anwar Hossain KM (2020) Arrowroot as bio-admixture for performance enhancement of concrete. J Build Eng. https://doi.org/10.1016/j.jobe.2020.101313
20. Sabbagh R, Esmatloo P (2019) Life cycle assessment for ordinary and frost-resistant concrete. In: Ameri F, Stecke K, von Cieminski G, Kiritsis D (eds) Advances in production management systems. Towards smart production management systems, vol 567. Springer, Cham. https://doi.org/10.1007/978-3-030-29996-5_19
21. Mbugua R, Salim R, Ndambuki J (2016) Effect of gum Arabic Karroo as a water-reducing admixture in cement mortar. Case Stud Constr Mater 5:100–111. https://doi.org/10.1016/j.cscm.2016.09.002
22. Akindahunsi AA, Uzoegbo HC (2015) Strength and durability properties of concrete with starch admixture. Int J Concr Struct Mater 9(3):323–335. https://doi.org/10.1007/s40069-015-0103-x
23. Akar C, Canbaz M (2016) Effect of molasses as an admixture on concrete durability. J Clean Prod 112:2374–2380. https://doi.org/10.1016/j.jclepro.2015.09.081
24. Hazarika A et al (2018) Use of a plant based polymeric material as a low cost chemical admixture in cement mortar and concrete preparations. J Build Eng 15:194–202. https://doi.org/10.1016/j.jobe.2017.11.017
25. Volf I, Ignat I, Neamtu M, Popa V (2014) Thermal stability, antioxidant activity, and photo-oxidation of natural polyphenols. Chem Pap 68(1). https://doi.org/10.2478/s11696-013-0417-6
26. Asante B, Appelt J, Yan L, Krause A (2023) Influence of wood pretreatment, hardwood and softwood extractives on the compressive strength of fly ash-based geopolymer composite. J Mater Sci 58(13):5625–5641. https://doi.org/10.1007/s10853-023-08371-0
27. Lootens D, Jousset P, Martinie L, Roussel N, Flatt RJ (2009) Yield stress during setting of cement pastes from penetration tests. Cem Concr Res 39(5):401–408. https://doi.org/10.1016/j.cemconres.2009.01.012
28. Lothenbach B, Durdzinski P, De Weerdt K (2016) Thermogravimetric analysis (A practical guide to microstructural analysis of cementitious materials). CRC Press, Cambridge
29. Scrivener K, Snellings R, Lothenbach B (2016) A practical guide to microstructural analysis of cementitious materials. CRC Press, Boca Raton
30. Peng Y, Zhang J, Liu J, Ke J, Wang F (2015) Properties and microstructure of reactive powder concrete having a high content of phosphorous slag powder and silica fume. Constr Build Mater 101:482–487. https://doi.org/10.1016/j.conbuildmat.2015.10.046
31. Wang L, Guo F, Lin Y, Yang H, Tang SW (2020) Comparison between the effects of phosphorous slag and fly ash on the C-S-H structure, long-term hydration heat and volume deformation of cement-based materials. Constr Build Mater. https://doi.org/10.1016/j.conbuildmat.2020.118807
32. Peniche-Pavía HA, Tzuc-Naveda JD, Rosado-Espinosa LA, Collí-Dulá RC (2024) FTIR-ATR chemometric analysis on pelagic *Sargassum* reveals chemical composition changes induced by cold sample transportation and sunlight radiation. J Appl Phycol 36(3):1391–1405. https://doi.org/10.1007/s10811-023-03167-w
33. Rosas-Díaz F, Martínez Arreguin A, Hernández JC, Juárez-Alvarado CA, Galindo-Rodríguez SA, García-Hernández DG (2025) Compatibility study of sargassum-based aggregate in Portland cement-based cementitious matrix. Revista de la construcción. https://doi.org/10.7764/rdlc.24.1.25

34. Pereira ALS et al (2014) Banana (*Musa* sp. cv. Pacovan) pseudostem fibers are composed of varying lignocellulosic composition throughout the diameter. BioResources 9(4):7749–7763
35. Xu S, Xiong C, Tan W, Zhang Y (2015) Microstructural, thermal, and tensile characterization of banana pseudostem fibers obtained with mechanical, chemical, and enzyme extraction. BioResources 10(2):3724–3735
36. Kumar N et al (2018) Optimal extraction, sequential fractionation and structural characterization of soda lignin. Res Chem Intermed 44(9):5403–5417. https://doi.org/10.1007/s11164-018-3430-0
37. Hernandez-Bolio GI, Fagundo-Mollineda A, Caamal-Fuentes EE, Robledo D, Freile-Pelegrin Y, Hernandez-Nunez E (2021) NMR metabolic profiling of *Sargassum* species under different stabilization/extraction processes. J Phycol 57(2):655–663. https://doi.org/10.1111/jpy.13117
38. Fares G, Al-Negheimish A, Alhozaimy AM, Khan MI (2022) Polycarboxylate superplasticizer and viscosity modifying agent: mode of addition and its effect on cement paste rheology using image analysis. J Build Eng. https://doi.org/10.1016/j.jobe.2021.103946
39. Roussel N, Bessaies-Bey H, Kawashima S, Marchon D, Vasilic K, Wolfs R (2019) Recent advances on yield stress and elasticity of fresh cement-based materials. Cem Concr Res. https://doi.org/10.1016/j.cemconres.2019.105798
40. Bessaies-Bey H et al (2018) Non-adsorbing polymers and yield stress of cement paste: effect of depletion forces. Cem Concr Res 111:209–217. https://doi.org/10.1016/j.cemconres.2018.05.004
41. Asakura S, Oosawa F (2003) Interaction between particles suspended in solutions of macromolecules. J Polym Sci 33(126):183–192. https://doi.org/10.1002/pol.1958.120331261 8
42. Yan Y, Wang R, Wang W, Yu C, Liu J (2021) Effect of starch-based admixtures on the exothermic process of cement hydration. Constr Build Mater. https://doi.org/10.1016/j.conbuildmat.2021.122903
43. Haas J, Nonat A (2015) From C-S-H to C-A-S-H: experimental study and thermodynamic modelling. Cem Concr Res 68:124–138. https://doi.org/10.1016/j.cemconres.2014.10.020
44. Garrault S (2005) Study of C-S-H growth on C3S surface during its early hydration. Mater Struct 38(278):435–442. https://doi.org/10.1617/14343
45. Skalny J, Maycock JN (1975) Mechanisms of acceleration by calcium chloride: a review. J Test Eval 3(4):303–311. https://doi.org/10.1520/jte10660j
46. Shi Z, Shi C, Liu H, Li P (2016) Effects of triisopropanol amine, sodium chloride and limestone on the compressive strength and hydration of Portland cement. Constr Build Mater 125:210–218. https://doi.org/10.1016/j.conbuildmat.2016.08.030
47. Pang X, Boul P, Cuello Jimenez W (2015) Isothermal calorimetry study of the effect of chloride accelerators on the hydration kinetics of oil well cement. Constr Build Mater 77:260–269. https://doi.org/10.1016/j.conbuildmat.2014.12.077
48. Chen H, Feng P, Ye S, Sun W (2018) The coupling effect of calcium concentration and pH on early hydration of cement. Constr Build Mater 185:391–401. https://doi.org/10.1016/j.conbuildmat.2018.07.067
49. Kunther W, Lothenbach B, Scrivener K (2013) Influence of bicarbonate ions on the deterioration of mortar bars in sulfate solutions. Cem Concr Res 44:77–86. https://doi.org/10.1016/j.cemconres.2012.10.016
50. Soria-Castro M, Genesca-Llongueras J, Hernandez-Bolio GI, Castro-Borges P (2024) Characterization of cement mortars with regional organic and inorganic additives. RSC Adv 14(22):15468–15482. https://doi.org/10.1039/d4ra00690a
51. Ekop I, Etim I-IN, Ambrose E, Edike UE (2024) Bio-based cement concrete admixtures for green recovery in the construction industry: a critical survey. Mater Circ Econ. https://doi.org/10.1007/s42824-024-00113-0
52. Venkatraman S, Ramasamy V (2019) Hydration effect of gum Arabic and guar gum powder on strength parameters of concrete. Caribb J Sci 53(2):124–133
53. Fang Y et al (2022) Bio-based admixture (Black Tea Extraction) for better performance of metakaolin blended cement mortars. Materials. https://doi.org/10.3390/ma15113994